Optical Magnus effect

A. V. Dooghin, N. D. Kundikova, V. S. Liberman, and B. Ya. Zel'dovich
Technical University, Chelyabinsk 454 080, U.S.S.R.
(Received 2 July 1991)

It is predicted theoretically and registered experimentally that the speckle pattern of a laser beam transmitted through a multimode fiber undergoes an angular shift from the switching of the chirality of the polarization. The effect may be considered as the result of the spin-orbit interaction for the photon in the inhomogeneous medium.

PACS number(s): 42.81.Gs, 42.25.Fx

INTRODUCTION

Looking at a rotating ping-pong ball falling through the air, we can seen that it is deflected from the vertical towards the direction of rotation due to the Magnus effect. If we assume that a circularly polarized photon propagating in a waveguide is like our rotating ball, we can expect its deviation from the initial trajectory.

It was shown by Rytov [1] and Vladimirskii [2] over 50 years ago that the plane of polarization undergoes some specific rotation connected with the nonplanar character (twisting) of the ray trajectory. Recently Chiao, Tomita, and Wu [3] found experimentally such a rotation in a single-mode optical fiber and treated it in terms of Berry's geometrical phase [4].

We are going to discuss an effect that may be considered to some extent as the inverse effect: rotation of the speckle pattern in multimode fiber due to the change of circular polarization from the left handed to right handed. In terms of quantum mechanics this effect can be regarded as an interaction between orbital momentum of a photon and its spin (polarization). Some preliminary theoretical and experimental results were recently published [5,6].

THEORY

Let us consider the propagation of light through an axially symmetrical fiber with a refractive-index profile $n(r)$:

$$n^2(r)=n_{co}^2[1-2\Delta S(r/\rho)] . \tag{1}$$

Here $(x,y)=\mathbf{r}$ are the transverse coordinates, $r=|\mathbf{r}|$, and ρ is the radius of the core, n_{co} and n_{cl} are the refractive indices of the core on the axis and of the cladding, respectively, $\Delta=(n_{co}^2-n_{cl}^2)/2n_{co}^2\approx\delta n/n_{co}\ll 1$ is the height parameter of the profile, $\delta n=n_{co}-n_{cl}$, and $S(r/\rho)$ is the profile: $S(0)=0$, $S(1)=1$.

The polarization is not coupled to the propagation of the beam in the zeroth-order paraxial approximation corresponding to the scalar parabolic equation. More accurately, the spatial structure of the field and its polarization are coupled due to inhomogeneity of the refractive index. The polarization correction to the propagation constant β of the mode $\mathbf{e}(\mathbf{r})\exp(i\beta z)$ in the first approximation has the form (see [7], Chap. 32, Eq. (32.24)):

$$\delta\beta=-\frac{(2\Delta)^{1/2}\rho}{2V}\frac{\int(\nabla_\perp\mathbf{e}_\perp)[\mathbf{e}_\perp^*\nabla_\perp\ln n^2(\mathbf{r})]d^2\mathbf{r}}{\int\mathbf{e}_\perp^*\mathbf{e}_\perp d^2\mathbf{r}} . \tag{2}$$

Here $\mathbf{e}(\mathbf{r})=\mathbf{e}_\perp(\mathbf{r})+e_z(r)\mathbf{e}_z$, $\nabla_\perp=\partial/\partial\mathbf{r}=\mathbf{e}_x(\partial/\partial x)+e_y(\partial/\partial y)$, $V=\rho k n_{co}(2\Delta)^{1/2}$ is a dimensionless parameter, $V\gg 1$ for a multimode fiber, $k=2\pi/\lambda$, and λ is the wavelength of the light in air.

The calculation of the corrections $\delta\beta$ requires the proper modes of the zeroth-order (uncoupled) approximation. Axial symmetry of the fiber allows one (see [7]) to take them in the following form:

$$\mathbf{e}_{m,N}^{\pm}(r,\varphi)=(1/\sqrt{2})(\mathbf{e}_x\pm i\mathbf{e}_y)\exp(im\varphi)F_{|m|,N}(r) \tag{3}$$

corresponding to right-handed and left-handed circular polarizations and the values of the orbital momentum $m=0,\pm2,\pm3,\pm4,\ldots$. Here $x=r\cos\varphi$, $y=r\sin\varphi$, $F_{|m|,N}(r)$ is the radial function, and $N=0,1,\ldots$ is the radial quantum number. It was shown [7] that for $m\neq\pm1$ just those modes constitute the proper basis for the diagonalization of a grad(n) perturbation.

It should be emphasized that in our approximation the circular polarization of the wave, right or left, is conserved during the propagation. The only modes which may violate that property are the ones with $m=+1$ or $m=-1$. We shall neglect their contribution in the subsequent consideration.

Analytical expressions for the polarization corrections may be explicitly obtained for the parabolic profile of the refractive index in the fiber, $S(r/\rho)=(r/\rho)^2$ for $r\leq\rho$. In that case the radial functions are

$$F_{|m|,N}(r)=(r/\rho)^{|m|}L_N^{|m|}(Vr^2/\rho^2)\exp(-Vr^2/2\rho^2) , \tag{4}$$

where $L_N^{|m|}$ are the generalized Laguerre polynomials. Then it follows from Eq. (2) that

$$\delta\beta_m^{\pm}=-\frac{\Delta\lambda}{2\pi\rho^2 n}(1\pm m) . \tag{5}$$

It is interesting to note that the correction (5) turned out to be independent of the radial quantum number N; this is a feature specific to the parabolic profile of the refractive index.

Suppose that we illuminate the fiber by right-hand circularly polarized light. Then the propagation results in

$$E^{+}(r,\varphi,z)=\frac{\mathbf{e}_x+i\mathbf{e}_y}{\sqrt{2}}\sum_m\sum_N C_{m,N}e^{im\varphi}F_{|m|,N}(r)\times\exp[iz(\beta_{mN}+\delta\beta^{+}_{mN})]\ . \quad (6)$$

An analogous expression may be obtained for the left-hand polarization.

Consider now an important specific case when we illuminate our fiber by right and left polarization in turn, but with strictly the same modal distribution $C_{m,N}$ at the input. It is interesting to compare the field and/or intensity distributions for $(\mathbf{e}_x+i\mathbf{e}_y)$ and $(\mathbf{e}_x-i\mathbf{e}_y)$ in some cross section z. Our qualitative analogy with the mechanical Magnus effect allows one to suppose that these distributions will be similar, but somewhat rotated around the fiber axis relative to each other.

That hypothesis may be verified most easily in the theory for the case of a fiber with a parabolic profile. In that case $\delta\beta^{\pm}_{mN}$ may be taken from Eq. (5), and therefore we see, that

$$E^{\pm}(r,\varphi,z)=\frac{\mathbf{e}_x\pm i\mathbf{e}_y}{\sqrt{2}}\sum_m\sum_N C_{m,N}\exp[im(\varphi\pm\kappa z)]F_{|m|,N}(r)\exp(iz\beta_{mN})\ , \quad (7)$$

where

$$\kappa=\frac{\Delta}{2\pi\rho^2 n}\lambda\ . \quad (8)$$

Equation (7) shows that the patterns $|\mathbf{E}^{\pm}(r,\varphi,z)|^2$ are the same, with mutual angular shift

$$\varphi_{+}-\varphi_{-}=2\kappa z\ . \quad (9)$$

There is a mnemonic rule to learn the sign of that shift. Let us consider the mechanical analogy with the rotation of a ping-pong ball, and the sign of its rotation will substitute for the sign of the electrical vector rotation for the light wave in a given cross section. The internal rotation of the ball (its spinning) results in the deviation of its trajectory after many rebounds from rough internal walls of our axially symmetric "ball guide." Then the sign of the deflection of the ball just corresponds to the sign of our optical effect.

If we take a step-index fiber, the analytical expressions cannot be obtained. Therefore we have calculated the modes and the corresponding corrections (2) by a computer for the particular fiber parameters: $n=1.5$, $\delta n=0.006$, $\lambda=0.63$ μm (He-Ne laser), and $2\rho=200$ μm.

It is important to note that for a general nonparabolic index profile the dependence of $\beta^{+}_{mN}-\beta^{-}_{mN}$ on m and N is rather complicated. Therefore the intensity patterns $|\mathbf{E}^{+}(r,\varphi,z)|^2$ and $|\mathbf{E}^{-}(r,\varphi,z)|^2$ will not be identical even for the same amplitudes of input modes. However, we can also expect that at some moderate propagation length those patterns will be somewhat similar to the relative angular shift of the same order of magnitude as in Eq. (9).

The radial functions in Eq. (2) are

$$\mathbf{e}^{\pm}_{m,N}(r,\varphi)=\begin{cases}\dfrac{\mathbf{e}_x\pm i\mathbf{e}_y}{\sqrt{2}}e^{im\varphi}J_{|m|}(Ur), & r/\rho<1 \quad (10a)\\ \dfrac{\mathbf{e}_x\pm i\mathbf{e}_y}{\sqrt{2}}e^{im\varphi}K_{|m|}(Wr), & r/\rho>1 \quad (10b)\end{cases}$$

for a step-index fiber. Here $J_{|m|}$ and $K_{|m|}$ are the Bessel and MacDonald functions, respectively, U and W ($V^2=W^2+U^2$) are determined from the equation

$$U\frac{J_{|m|+1}(U)}{J_{|m|}(U)}=W\frac{K_{|m|+1}(W)}{K_{|m|}(W)}\ . \quad (11)$$

Polarization corrections due to (2) are

$$\delta\beta^{+}_{|m|,N}=\delta\beta^{-}_{-|m|,N}=\frac{(2\Delta)^{3/2}}{2\rho}\frac{WU^2}{V^3}\frac{K_{|m|}(Wr)}{K_{|m|+1}(Wr)}\ , \quad (12a)$$

$$\delta\beta^{-}_{|m|,N}=\delta\beta^{+}_{-|m|,N}=\frac{(2\Delta)^{3/2}}{2\rho}\frac{WU^2}{V^3}\frac{K_{|m|}(Wr)}{K_{|m|-1}(Wr)}\ . \quad (12b)$$

These equations were used for the numerical modeling of our physical experiment.

COMPUTER EXPERIMENT

Phase-constant and polarization corrections are shown in Figs. 1 and 2 versus the modal indices m and N. It is seen from Fig. 1 that our waveguide confines the modes with $m\leq 129$ and $N\leq 44$. However only the modes with $m\leq 60$ and $N\leq 20$ which corresponded to the real parameters of the speckle pattern in physical experiment were used for the numerical simulation. Complex amplitudes $C_{m,N}$ for the specific realization of the speckle pattern in Eq. (6) were obtained by the random number generator. Figure 3 shows the angular distribution of speck-

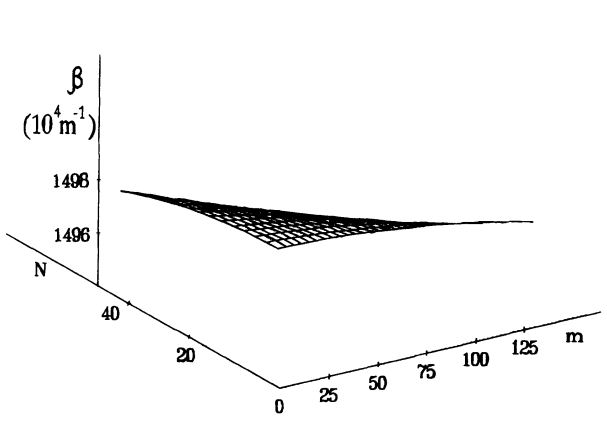

FIG. 1. Propagation constants vs mode indices calculated for the step-index fiber with $2\rho=200$ μm, $n_{co}=1.5$, $\delta n=0.006$ in scalar approximation.

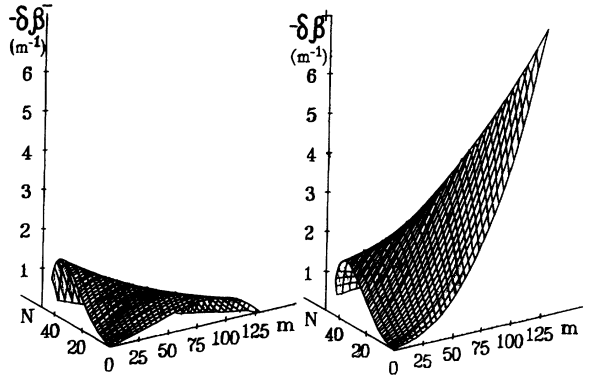

FIG. 2. Polarization corrections to the propagation constants vs mode indices calculated for the step-index fiber with $2\rho=200$ μm, $n_{co}=1.5$, $\delta n=0.006$.

le patterns $|\mathbf{E}^{\pm}(r,\varphi,z)|^2$ for one particular realization at a given radius for the left and right circular polarizations. It is readily seen from Fig. 3 that under the change of circular polarization all patterns undergo an angular shift (rotation); but the main features are intact, although slightly distorted. The angular shift is about 1.5°.

To extract the pure rotation change from the whole change of the speckle pattern we have calculated the correlation functions:

$$K_{ij}(r,\psi,z)=\int I_i(r,\varphi,z)I_j(r,\varphi+\psi,z)d\varphi\ ,$$
$$I_i(r,\varphi,z)=|\mathbf{E}^i(r,\varphi,z)|^2,\quad i=+,-;\quad j=+,-\ . \tag{13}$$

Hence, averaging over the statistical ensemble was substituted by the averaging over the angle φ in interval $0<\varphi<2\varphi_0$ with $\varphi_0\gg\pi/m_{\max}$, $2\varphi=360°$. The effect we are seeking manifests itself in the sharp maximum of the correlation function $K_{+-}(\psi)$ at some definite value of $\psi_0\neq0$, which is just our rotation angle, $\psi_0=\varphi_+-\varphi_-$.

The autocorrelation function for left-handed circular polarization $K_{--}(\psi)$ and cross-correlation functions $K_{+-}(\psi)$ for different radii and realizations are presented

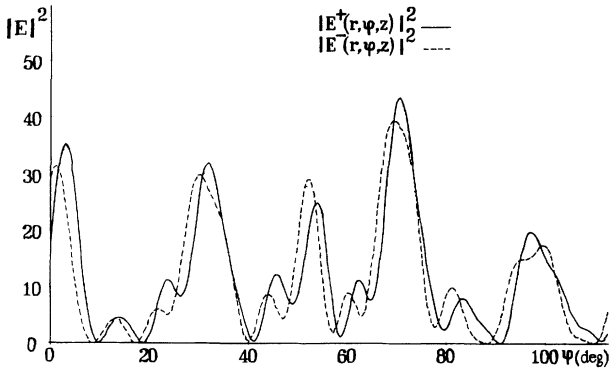

FIG. 3. Angular profile of the speckle patterns $|\mathbf{E}^i(r,\varphi,z)|^2$ of right-hand ($i=$"+") and left-hand ($i=$"−") circularly polarized light at a given fiber length $z=96$ cm and radius $r=\rho/2$.

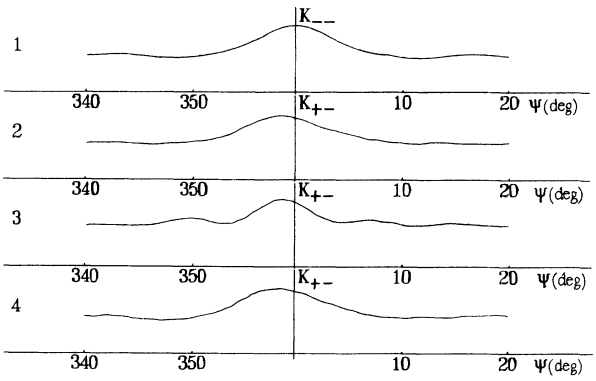

FIG. 4. Autocorrelation function $K_{--}(r,\psi,z)$ (1) and correlation functions $K_{+-}(r,\psi,z)$ (2,3,4) versus the angular shift ψ between the speckle patterns at a given fiber length $z=96$ cm for different radii and realizations. 1,2,4 denotes $r=\rho/2$; 3 denotes $r=0.8\rho$; 1,3,4 denotes the first realization; 2 denotes the second realization.

in Fig. 4. In Fig. 5 we show the correlation functions for different fiber lengths. As we expected, the correlation function had a sharp maximum at the angle $\psi_0\neq0$, which was proportional to the length, and at $z=96$ cm was equal to 1.5° independent of the radius and specific realization. It is interesting to note that the modulation depth of the correlation function corresponds to the case of complex Gaussian statistics.

EXPERIMENT

Unfortunately, in the setup with the fiber having the parabolic refractive-index profile, the linear polarization was not conserved at a reasonable distance. That is why we carried out an experiment with a step-index fiber with the next parameters: $2\rho=200$ μm; the difference between refractive indices of quartz core and polymeric cladding $\Delta n=n_{co}-n_{cl}=0.006$ was measured via the critical angle of propagating rays.

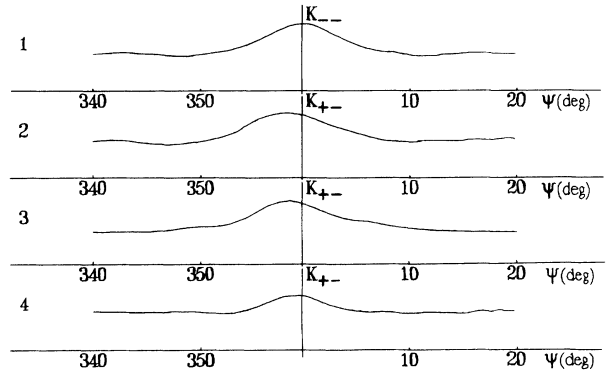

FIG. 5. Autocorrelation function $K_{--}(r,\psi,z)$ (1) and correlation functions $K_{+-}(r,\psi,z)$ (2,3,4) vs the angular shift ψ between the speckle patterns at a given radius $r=\rho/2$ for the different fiber lengths: $z=96$ cn (1,2), $z=72$ cm (3), and $z=48$ cm (4).

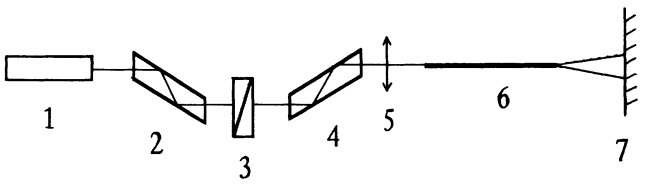

FIG. 6. Experimental setup. 1 denotes the He-Ne laser with linear polarization and wavelength $\lambda=0.63$ μm; 2,4 denote the Fresnel rhombi; 3 denotes the polarizer; 5 denotes the lens; 6 denotes the fiber under investigation; 7 denotes the screen with the polar coordinate net.

The experimental setup is shown in Fig. 6. The beam of He-Ne laser 1 with linear polarization and wavelength $\lambda=0.63$ μm propagated through the Fresnel rhomb 2. The plane of linear polarization was oriented in such a way that the outgoing radiation was circularly polarized. Polarizer 3 allowed us to separate the desirable linear polarization from the circular one. Furthermore, the light propagated through the second Fresnel rhomb 4. By lens 5 the light was focused at the entrance of fiber 6. The rotation of polarizer 3 at 90° allowed us to switch from the left-handed circular polarization of the propagating beam to the right-handed polarization and back. The speckle pattern of the light transmitted by the fiber was observed at screen 7 with the polar coordinate net.

At first we examined the polarization properties of our fiber. It turned out that the linear polarization was conserved at a distance of about 20–30 cm fiber length. But we did not see the effect we desired at such a length. After propagation through 2 m of fiber length the radiation was strongly depolarized and the perturbation of the speckle pattern due to the polarization sign change seemed to be irregular.

The 1-m-long fiber conserved linear polarization, in general, but a small part of the radiation was depolarized. Considering that case as the most favorable we took the 96-cm-long fiber for our experiment.

We were able to measure the rotation of linear polarization of the light transmitted through a fiber, the latter having been coiled in a type of helix. The angle of that rotation corresponded to the results of Rytov [1], Vladimirskii [2], Berry [4], and Chiao, Tomita, and Wu [3] (see also [8,9]). It is important to note that this angle, together with the degree of output linear polarization ($>85\%$), did not depend on orientation of the input linear polarization. This finding is indirect evidence for the absence of internal stress and birefringence in the fiber.

However, for our main experiments on the optical Magnus effect we kept the 96-cm piece of fiber rectilinear and freely laying on a plane support.

Actually, by changing the circular polarization of propagating light from left handed to right handed we could see the pattern moving clockwise in accordance with the theoretical prediction. During that motion some details of the speckle pattern changed, but the main features were conserved under rotation. It may be seen in Fig. 7: the fragments of the speckle patterns for both circular polarizations are shown as they are seen at the screen. The arrow points to the bright spot that was rotated slightly, changing its shape (just as in the computer experiment, see Fig. 3)].

We did our best to eliminate possible sources of systematic errors. One of them could be caused by the change of the wave front of the beam at the fiber input at the switch of polarization from right to left. To look into this possibility, we performed the same switching, but with an additional linear polarizer just before the fiber input. We did not see any changes of the output speckle pattern under that switching in such conditions. It means that the wave front was not changed by the switch of circularity.

It would be helpful to measure the intensity correlation function versus angular shift. Unfortunately we did not have adequate equipment to measure the amount of pix-

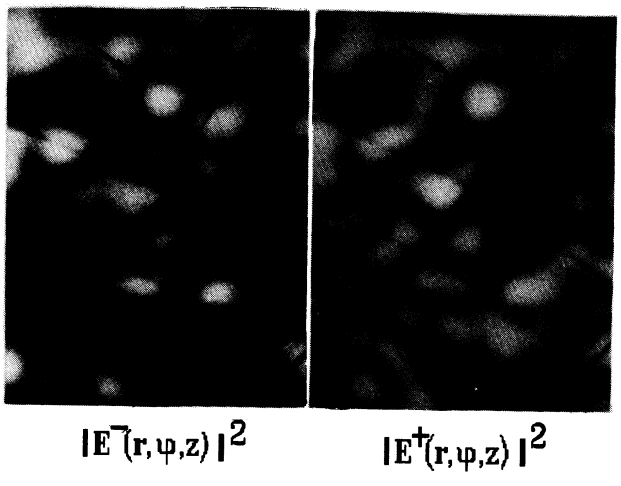

FIG. 7. The fragment of the real speckle patterns $|E^{i}(r,\varphi,z)|^2$ of right-hand ($i=+$) and left-hand ($i=-$) circularly polarized light at the screen. The arrows points to the bright spot as an example of rotation under circular polarization sign change.

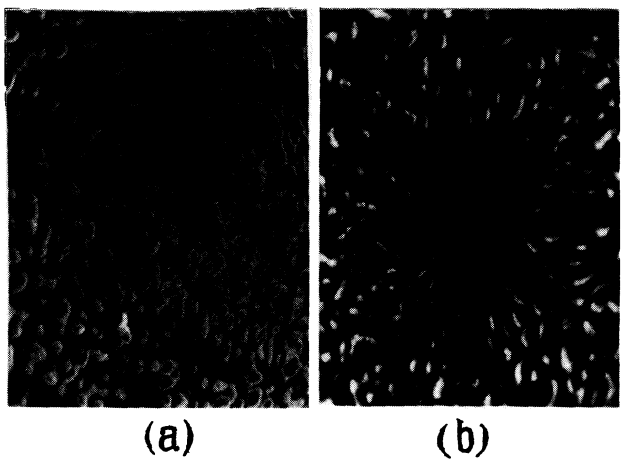

FIG. 8. The slide with the negative image of the speckle pattern projected onto its own positive photograph: (a) both coordinate nets coincide; (b) coordinate nets are mutually rotated at the angle $\psi\approx4°$.

els of the image of the two-dimensional speckle pattern. Therefore for more accurate measurement of the "rotation angle," we used an experimental analog of the correlation-function technique. Projecting the slide with the negative image of the speckle pattern against its own positive photograph, we obtain the least contrast of the whole picture under the coincidence of both coordinate nets [see Fig. 8(a)]. Even slight mutual rotation yields a sharp increase of the contrast [see Fig. 8(b)]. It approximately corresponds to the autocorrelation function shown in Fig. 4. For the rotation-angle measurement we projected a negative slide for the right-handed circular polarization speckle pattern onto the positive photograph of the left-handed one and achieved the least contrast by their mutual rotation. The angle between the two coordinate nets corresponding to the contrast minimum was regarded as the "rotation angle." For our fiber it was 1.4°. By repeating this measurement several times, we found the same result with an accuracy of $\pm 0.5°$.

CONCLUSION

The coincidence of the theoretically computed rotation $+1.5°\pm 0.5°$ with the experimentally measured rotation $+1.4°\pm 0.5°$ proved to be incredibly good. Even the analytical result for the fiber with the parabolic profile of the refractive index gives quite a reasonable estimation ($+3.3°$) for the effect.

This convinces us that we have predicted and observed the optical Magnus effect, i.e., the rotation of the image transmitted through a fiber under the switch of the chirality of light polarization.

ACKNOWLEDGMENTS

We are grateful to V. V. Shkunov for valuable discussion and to Z. A. Baskakova for the fiber in which the effect was observed.

[1] S. M. Rytov, Dokl. Acad. Nauk. U.S.S.R. **18**, 2 (1938).
[2] V. V. Vladimirskii, Dokl. Acad. Nauk. U.S.S.R. **21**, 222 (1941).
[3] R. Y. Chiao, A. Tomita, and Y.-S. Wu, in *Geometric Phases in Physics,* edited by A. Shapere and F. Wilczek (World Scientific, Singapore, 1989).
[4] M. V. Berry, Proc. R. Soc. London Ser. A **392**, 45 (1984).
[5] B. Ya. Zel'dovich and V. S. Liberman, Kvantovaya Elektron. (Moscow) **17**, 493 (1990) [Sov. J. Quantum Electron. **20**, 427 (1990)].
[6] B. Ya. Zel'dovich, A. V. Dooghin, N. D. Kundikova, and V. S. Liberman, Pis'ma Zh. Eksp. Teor. Fiz. **53**, 186 (1991) [Sov. Phys. JETP Lett. **53**, 197 (1991)].
[7] A. W. Snyder and J. D. Love, *Optical Waveguide Theory* (Methuen, London, 1984).
[8] R. Y. Chiao, A. Antaramian, K. M. Canga, H. Jiao, and S. R. Wilkinson, Phys. Rev. Lett. **60**, 1214 (1988).
[9] H. Jiao, S. R. Wilkinson, R. Y. Chiao, and H. Nathel, Phys. Rev. A **39**, 3475 (1989).

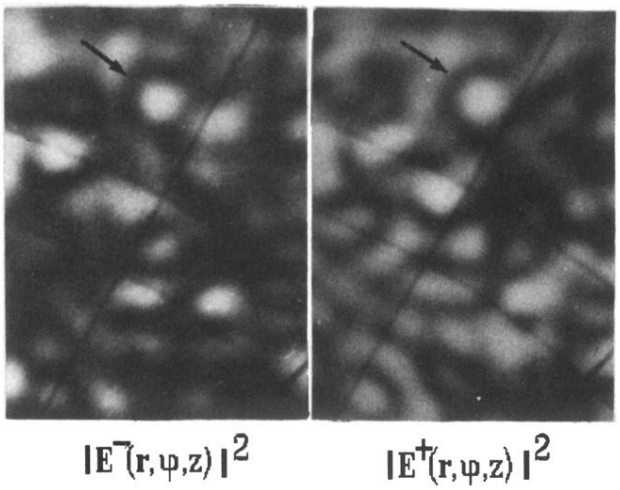

FIG. 7. The fragment of the real speckle patterns $|\mathbf{E}^i(r,\varphi,z)|^2$ of right-hand ($i=+$) and left-hand ($i=-$) circularly polarized light at the screen. The arrows points to the bright spot as an example of rotation under circular polarization sign change.

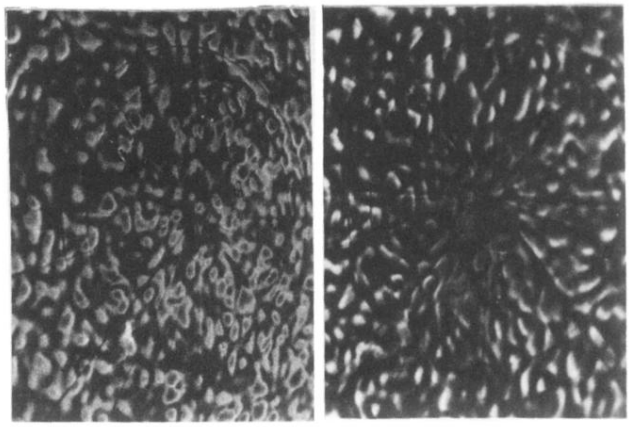

FIG. 8. The slide with the negative image of the speckle pattern projected onto its own positive photograph: (a) both coordinate nets coincide; (b) coordinate nets are mutually rotated at the angle $\psi \approx 4°$.